

Article

A Highly Efficient Fluorescent Sensor Based on AIEgen for Detection of Nitrophenolic Explosives

Dongmi Li ^{1,*}, Panpan Lv ^{2,†}, Xiao-Wen Han ², Zhilei Jia ¹, Min Zheng ¹ and Hai-Tao Feng ^{2,*}

¹ Henan Key Laboratory of Function-Oriented Porous Materials, College of Chemistry and Chemical Engineering, Luoyang Normal University, Luoyang 471000, China

² AIE Research Center, College of Chemistry and Chemical Engineering, Baoji University of Arts and Sciences, Baoji 721013, China

* Correspondence: lidongmi223@126.com (D.L.); haitaofeng907@163.com (H.-T.F.)

† These authors contributed equally to this work.

Abstract: The detection of nitrophenolic explosives is important in counterterrorism and environmental protection, but it is still a challenge to identify the nitroaromatic compounds among those with a similar structure. Herein, a simple tetraphenylethene (TPE) derivative with aggregation-induced emission (AIE) characteristics was synthesized and used as a fluorescent sensor for the detection of nitrophenolic explosives (2, 4, 6-trinitrophenol, TNP and 2, 4-dinitrophenol, DNP) in water solution and in a solid state with a high selectivity. Meanwhile, it was found that only hydroxyl containing nitrophenolic explosives caused obvious fluorescence quenching. The sensing mechanism was investigated by using fluorescence titration and ¹H NMR spectra. This simple AIE-active probe can potentially be applied to the construction of portable detection devices for explosives.

Keywords: fluorescence probe; aggregation-induced emission; trinitrophenol; explosives



Citation: Li, D.; Lv, P.; Han, X.-W.; Jia, Z.; Zheng, M.; Feng, H.-T. A Highly Efficient Fluorescent Sensor Based on AIEgen for Detection of Nitrophenolic Explosives. *Molecules* **2023**, *28*, 181. <https://doi.org/10.3390/molecules28010181>

Academic Editors: Li-Ya Niu and Xuewen He

Received: 17 November 2022

Revised: 20 December 2022

Accepted: 21 December 2022

Published: 25 December 2022



Copyright: © 2022 by the authors. Licensee MDPI, Basel, Switzerland. This article is an open access article distributed under the terms and conditions of the Creative Commons Attribution (CC BY) license (<https://creativecommons.org/licenses/by/4.0/>).

1. Introduction

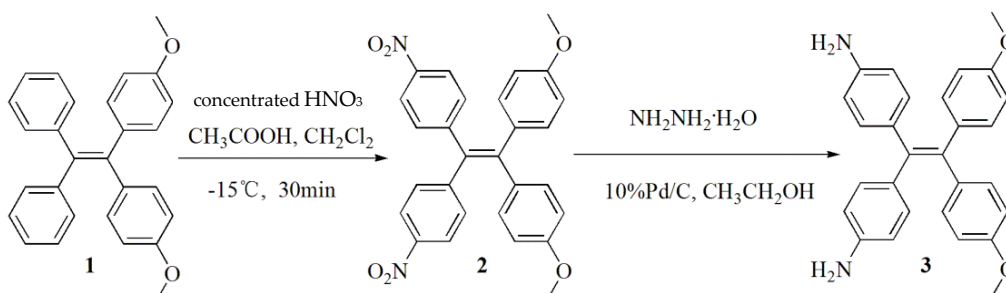
The effective detection of nitroaromatic compounds (NACs) is of great importance in modern society owing to their threats to both national security and environmental safety. Different nitroaromatic explosives such as 2, 4, 6-Trinitrophenol (TNP, picric acid) and 2, 4-dinitrophenol (DNP) are broadly utilized in the assembling of rocket fills, firecrackers, matches, etc. Additionally, TNP and its derivatives are also used in the field of medical formulation as an antiseptic agent, as well as being used as a yellow pigment in dye and leather industries, which will cause environmental pollution and health hazards [1,2]. Consequently, the development of highly selective and sensitive sensors with a quick response for discriminating TNP and DNP is imperative for natural remediation, regular citizen security, and military tasks.

Presently, several analytical techniques have been developed for the detection of nitroaromatic explosives, such as trained canines [3], mass spectrometry [4], gas chromatography [5,6], liquid chromatography [7], ion mobility spectrometry [8], electrochemical assay [9], high performance liquid chromatography [10], X-ray imaging, Raman spectroscopy [11], and so on. In contrast to the above-mentioned methods, fluorescent probes with the merits of high sensitivity, selectivity, easy visualization, and a short response time have attracted great attention in various areas [12–16]. To date, numerous fluorescent sensors based on polymers [17,18], metal–organic frameworks [19], fluorescent quantum dots [20,21], and organic small molecules [13] have been designed and developed. Despite these advances, most of the traditional fluorophores have often encountered the aggregation-caused quenching (ACQ) problem in the aggregated state, which has been a hurdle to fluorescence sensing. Moreover, selective detection of nitroaromatic explosives remains difficult due to their similar electron affinity.

Since aggregation-induced emission (AIE) was termed by Tang in 2001 [22], a large number of AIE luminogens (AIEgens) have been developed for photoelectric devices, biomaterials and fluorescent probes [23–27]. Thanks to their high sensitivity and solid-state emission efficiency, detection of explosives based on AIE-active probes has received a lot of interest [28–32]. Among these AIEgens, tetraphenylethene (TPE) is the most popular building block for the construction of fluorescence sensors due to its high photostability, simple synthesis, and easy structure modification. For example, Tang and their co-workers reported that a series of TPE-based polymers can serve as highly sensitive sensors for TNP through a mode of emission quenching with this substrate [33–36]. To provide the fluorescence sensors with better selectivity, the Zheng group designed several TPE-based macrocycles showing a high selectivity for NACs, alongside the excellent sensitivity by virtue of the encapsulation [37–39]. Throughout the course of our continuous effort to develop an excellent fluorescence probe for explosives, herein a simple TPE-based AIEgen was synthesized to detect TNP from a series of NACs. Such material showed highly sensitive fluorescence quenching to TNP in aqueous solution and in a solid state by virtue of photo-induced electron transfer. This simple AIE-active probe can potentially be applied to the construction of portable detection devices for explosives.

2. Results and Discussion

The synthetic procedure of the target compound **3** was designed and presented in Scheme 1. The known tetraphenylethene derivative **1** was utilized as the starting material. It was then nitrated by concentrated nitric acid and acetic acid in dichloromethane to afford molecule **2**. By a reduction of **2** with hydrazine hydrate and Pd/C in ethanol, the target molecule **3** was obtained in a good yield of 87%. The molecule **3** was fully characterized by ^1H NMR, ^{13}C NMR, high resolution mass spectra (HRMS), and infrared (IR) spectra in the Supporting Information (Figures S1–S4).



Scheme 1. Synthetic route of compound **3**.

The photophysical properties of compound **3** were then investigated. The UV/Vis absorption spectra of **3** responding to TNP were measured in dimethylsulfoxide (DMSO). The molecule **3** showed absorption bands at 342, 292 and 261 nm. When adding TNP to **3**, the absorption intensity largely increased, but the algebraic sum of spectrum of **3** and the spectrum of TNP is similar to the spectrum of the mixture of **3** + TNP, implying that there were weak interactions in the solution state (Figure S5). From the photoluminescence (PL) spectra we can see that compound **3** was non-emissive in THF (Figure 1). Upon the addition of poor solvent water to THF, the solution remained weak in fluorescence from 0 to 80% water fraction. Upon further enhancing the water fraction to 92%, compound **3** emitted bright blue fluorescence at 478 nm. The 58-fold enhancement of PL intensity indicated that compound **3** is an AIE-active compound. The scanning electron microscope (SEM) images revealed that the turbid solution of **3** in 92% water fraction was composed of many rod-like aggregates with the length of micrometers (Figure S6).

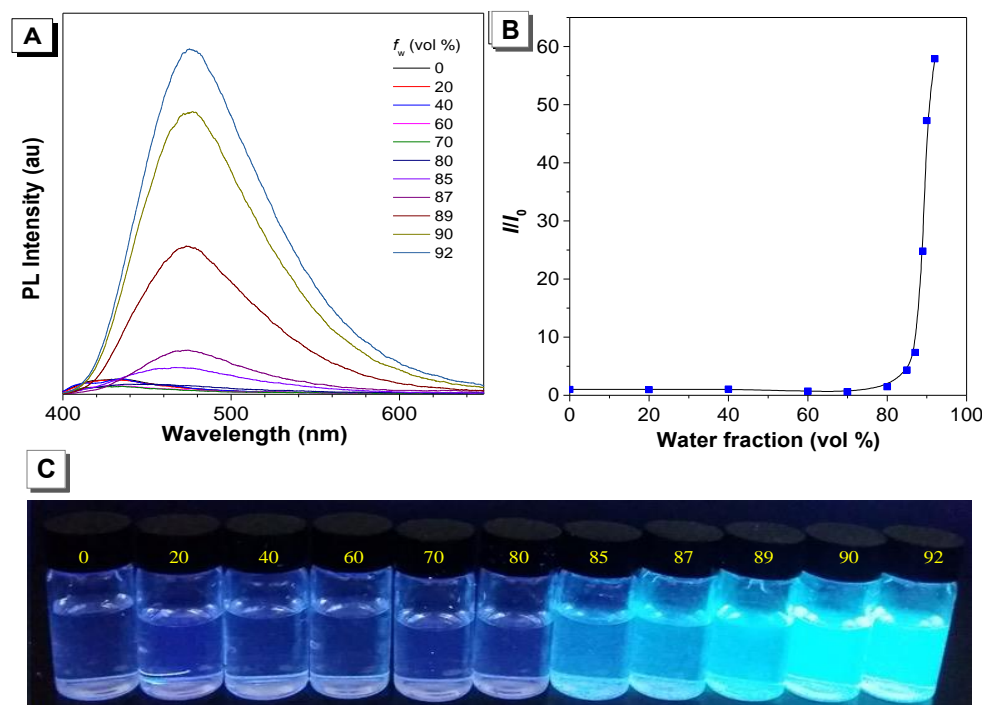


Figure 1. (A) Fluorescence spectra of compound **3** (5.0×10^{-5} M) in THF with different water fractions. $\lambda_{\text{ex}} = 340$ nm, ex/em slit widths = 5/5 nm. (B) PL intensity ratio of I/I_0 in different THF/H₂O mixtures. (C) Fluorescent images of compound **3** (5.0×10^{-5} M) with changing water fractions from 0 to 92% in THF under a 365 nm UV lamp.

The fluorescence response of molecule **3** to NACs was then studied in H₂O/THF (9: 1, v/v). As shown in Figure 2A, molecule **3** (20 μ M) fluoresced strongly in 90% water fraction without NACs. When different nitrophenolic explosives (40 μ M) were added into the solution, such as 2,4,6-trinitrophenol (TNP), 2,4-dinitrophenol (DNP), *p*-nitrophenol (PNP), *o*-nitrophenol (ONP), 2,4,6-trinitromethylbenzene (TNT), 2,4-dinitrotoluene (DNT), *p*-nitrotoluene (PNT), *o*-nitrotoluene (ONT), nitrobenzene (NB), 1,3-dinitrobenzene (DNB), 1-fluoro-2,4-dinitrobenzene (DNFB), 4-hydroxyisophthalonitrile (HPN), 2,4-dinitrochlorobenzene (DNCB), 3-cyanopheno (CP), phenol, 3,5-dinitrobenzoic acid (DNA), and 2-Hydroxybenzonitrile (HBN), the sharp quenching caused by TNP and DNP was observed under a 365 nm UV light. Meanwhile, it was found that only hydroxyl containing nitrophenolic explosives caused obvious fluorescence quenching, while other NACs showed a minor influence on the emission of molecule **3**. The quenching efficiency of PNP, ONP, DNP, and TNP increased with the enhancement of acidity. Therefore, it is inferred that the existence of electrostatic interactions led to the high selectivity of molecule **3** to TNP and DNP. The quenching efficiency ($(1 - I/I_0) \times 100\%$) of compound **3** for TNP and DNP were 95% and 79%, respectively (Figures 2B and S7).

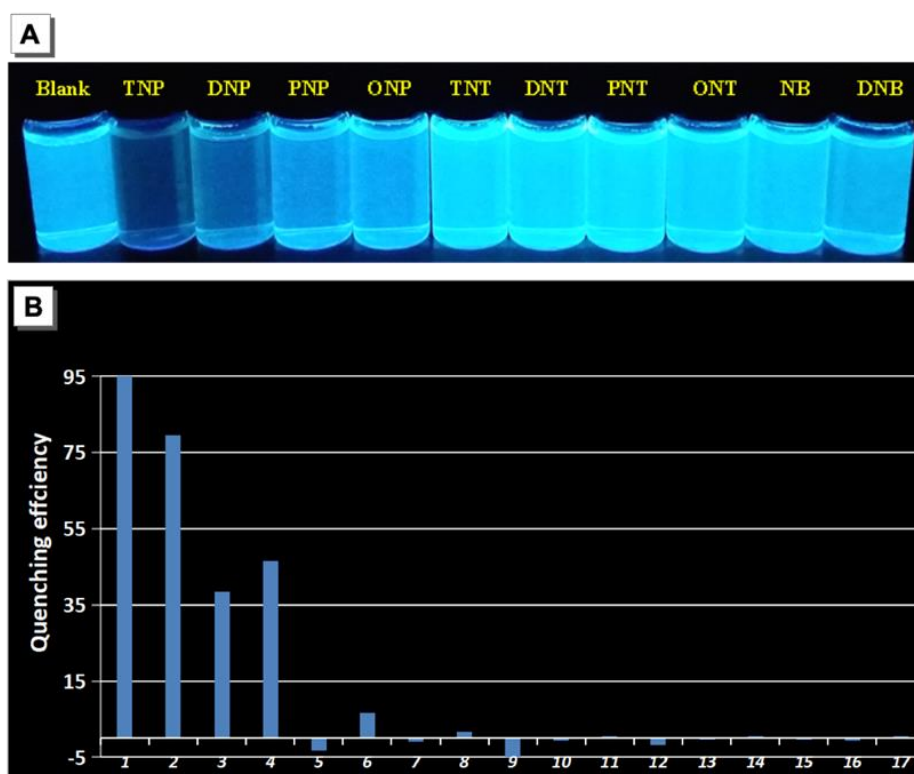


Figure 2. (A) Fluorescent images of compound **3** with various nitrophenolic explosives under a 365 nm UV lamp. (B) The Fluorescence quenching efficiencies ($(1 - I/I_0) \times 100\%$), where I and I_0 denote the fluorescence intensity of compound **3** with and without analytes, respectively. 1: TNP, 2: DNP, 3: PNP, 4: ONP, 5: TNT, 6: DNT, 7: PNT, 8: ONT, 9: NB, 10: DNB, 11: DNFB, 12: HPN, 13: DNCB, 14: 3-Cyanopheno, 15: Phenol, 16: DNA, 17: HBN. Solvent: H₂O: THF = 9: 1, [3] = [explosives]/2 = 2×10^{-5} M. $\lambda_{\text{ex}} = 340$ nm, ex/em slit widths = 5/5 nm.

The fluorescence titration of **3** (20 μM) with different equivalents of TNP was measured to verify their complexation ratio. As shown in Figure 3A, the PL intensity of molecule **3** at 460 nm gradually decreased when the TNP concentration was increased to 40 μM . The stoichiometry between compound **3** and TNP was calculated from Job's plot to be 1: 2 (Figure 3B). Based on the data presented in Figure S8, the association constant was estimated to be 3.4×10^8 from linear curve fitting using Origin software [40,41]. Similar results were obtained from the fluorescence titrations of **3** with DNP (Figure 3C). The stoichiometry from Job's plot was estimated to be 1:2 also (Figure 3D) and the association constant was calculated to be 7.4×10^7 (Figure S9). From the association constants we can conclude that molecule **3** has much a stronger affinity to TNP than DNP. Due to the higher number of electron-withdrawing nitro groups in TNP, it exhibited much more acidity than other nitrophenolic compounds. Thus, it is easy to form complexes with molecule **3** to occur photo-induced electron transfer within the complex resulting in fluorescence quenching. Then fluorescence lifetimes of compound **3**, TNP, and the mixture of compound **3** + TNP were measured in an aqueous solution to verify their interactions. As illustrated in Figure S10, compound **3** gave a lifetime of 4.52 ns. Upon the addition of TNP to the system, the lifetime reduced to 0.35 ns, indicating the existence of static fluorescence quenching.

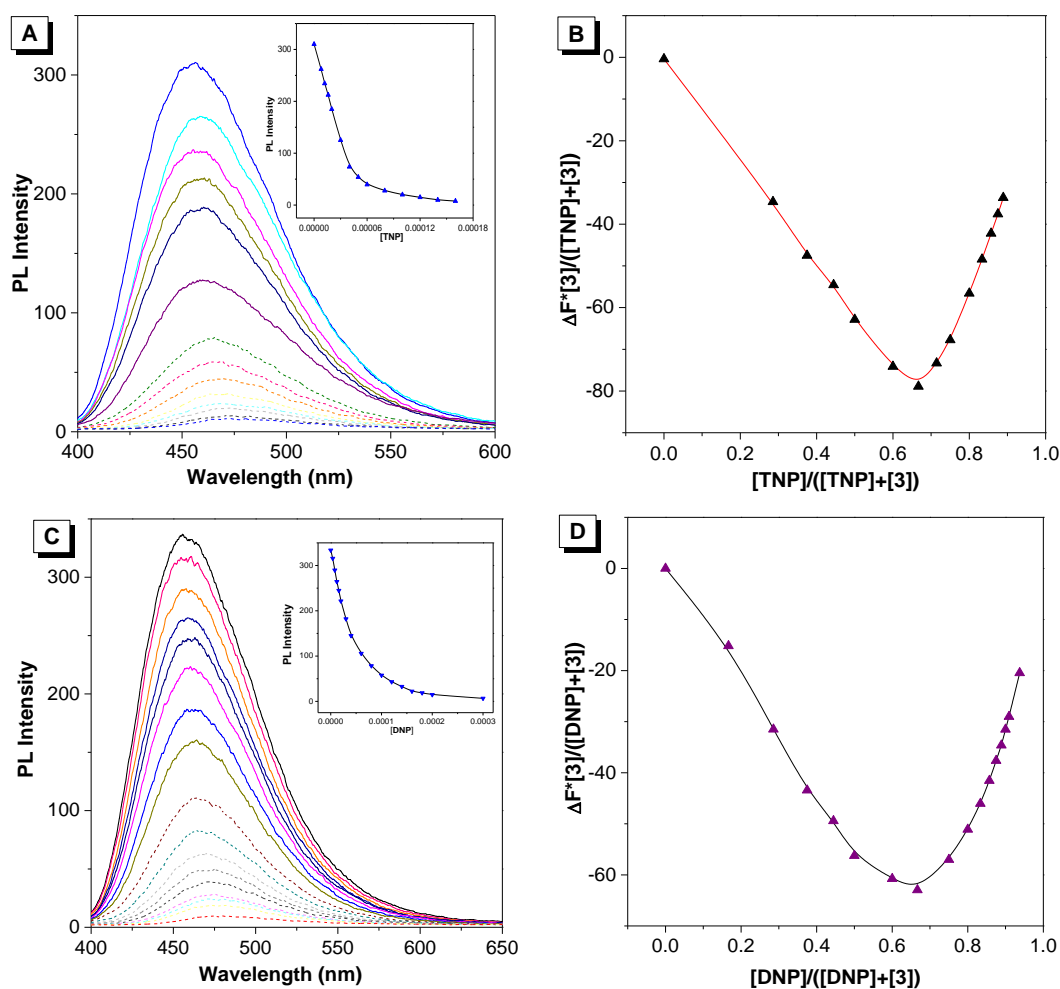


Figure 3. (A) The PL spectra of compound 3 with different amounts of TNP. Solvent: H₂O: THF = 9: 1, [3] = 2 × 10⁻⁵ M, [TNP] = 0–1.6 × 10⁻⁴ M. Inset: the PL change was observed at 460 nm when compound 3 was combined with TNP. (B) The Job's plot of compound 3 (2 × 10⁻⁵ M) with TNP at 460 nm. (C) The PL spectra of compound 3 with different amounts of DNP. Solvent: H₂O: THF = 9: 1, [3] = 2 × 10⁻⁵ M, [DNP] = 0–3 × 10⁻⁴ M. Inset: compound 3 fluorescence intensity variation with TNP content at 460 nm. (D) The Job's plot of compound 3 (2 × 10⁻⁵ M) with DNP at 460 nm. λ_{ex} = 340 nm, ex/em slit widths = 5/5 nm.

¹H NMR titration in *d*₆-DMSO was performed again to gain a deeper understanding of the bond formation between compound 3 and TNP. In fact, we made an attempt to record the NMR titration in the mixture of deuterated water and THF with 90% deuterated water fraction. Unfortunately, the compound 3 and TNP could not dissolve in the mixed solvents. Thus, we carried out ¹H NMR titration in *d*₆-DMSO. As shown in Figure 4A, when two equivalents of TNP were added, the chemical shift H_a of compound 3 showed a downfield shift from 6.26 to 7.01 ppm. Upon further addition of TNP, the chemical shift was only slightly altered. Additionally, there was also an obvious downfield shift of H_b in compound 3 from 6.58 to 7.02 ppm. These results proved that the electrostatic interaction between amino groups and hydroxyl group mainly contributes to the binding between TNP and compound 3. ¹H NMR titration indicated that a 1:2 binding ratio was obtained between compound 3 and TNP as shown in Figure S11. It is worth noting that this binding ratio was obtained from a *d*₆-DMSO concentrated solution (5 mM) in ¹H NMR titration and it is not clear if this will also be true with its diluted solution in H₂O: THF (90% water fraction), with concentration of the order 10⁻⁵ M. However, from the results of ¹H NMR and fluorescence

titration we can see that they obtained the same complexation ratio. Additionally, Figure 4B illustrates a possible binding mode between compound 3 and TNP.

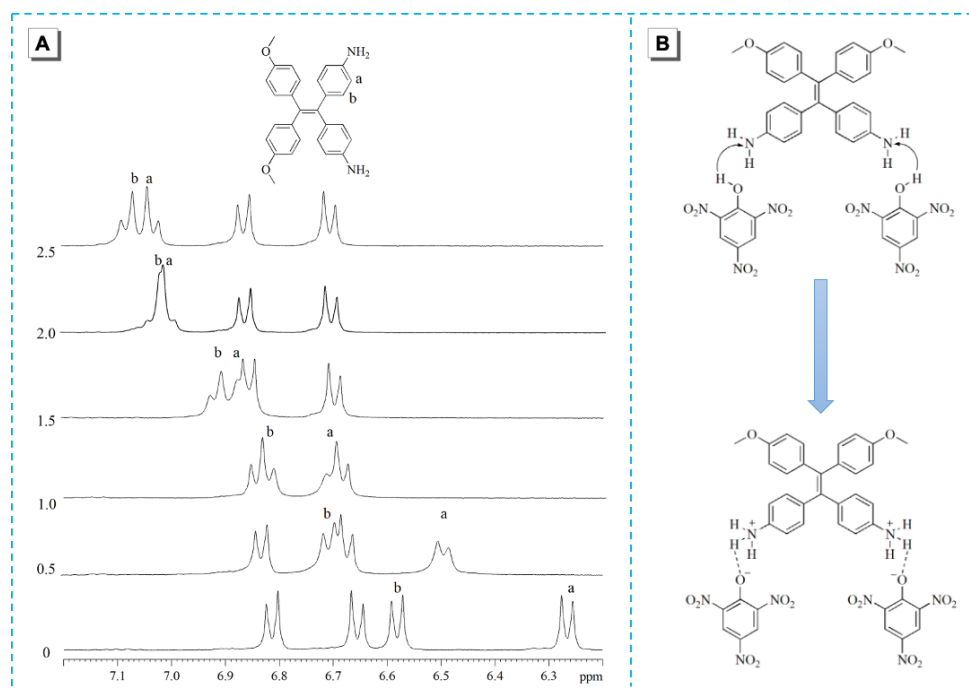


Figure 4. (A) Changes of ^1H NMR spectra of compound 3 (5 mM) in d_6 -DMSO with the addition of TNP. (B) The possible binding mode of compound 3 with TNP.

Furthermore, fluorescence detection of TNP was also estimated in the solid state (Figure 5). Compound 3 was dripped onto the TLC plate and dried under a vacuum. The TLC plate with pure compound 3 showed bright fluorescence. When different concentrations of TNP solution were dripped on the spot of compound 3, the fluorescence was quickly quenched. From the picture we can see that 0.2 μM of compound 3 can cause obvious fluorescence quenching on the TLC plate. The data verified that compound 3 is an excellent sensor for TNP not only in the solution, but also in the solid state.

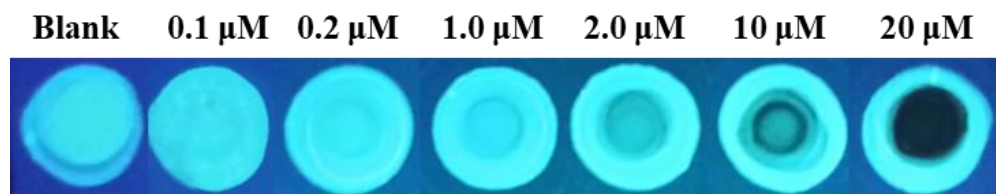


Figure 5. Fluorescent photographs of compound 3 with and without TNP solution on the TLC plate under 365 nm UV light.

3. Materials and Methods

Materials: All reagents and solvents were chemical pure (CP) grade or analytical reagent (AR) grade and were used as received.

Measurements: ^1H and ^{13}C NMR were measured on 400 MHz Bruker Advanced III (Bremen, Germany). Mass spectrum was measured on Waters instrument (Framingham, MA, USA). IR was measured on Bruker VERTEX70 (Bremen, Germany). Fluorescent spectra were collected on Hitachi F-4500 spectrophotometer (Tokyo, Japan).

3.1. Synthesis of 2

The mixture of 30 mL dichloromethane, 2.85 mL (40.9 mmol) concentrated nitric acid, and 2.34 mL (20.8 mmol) acetic acid was added to a 100 mL drying flask. The flask was placed in a low temperature reaction bath at $-15\text{ }^{\circ}\text{C}$, 2 g 4, 4'-dimethoxytetraphenylethene (5 mmol) was added to the mixture under stirring for 0.5 h. The reaction mixture was taken out of the low-temperature reaction bath and returned to room temperature. The product was quenched by adding 20 mL of water. The organic phase was separated and washed with water several times until the pH was 7. Compound 2 was obtained as a yellow solid by evaporating the solvent using a rotary evaporator (1.95 g, 81%).

3.2. Synthesis of 3

Compound 2 (1 g, 2.1 mmol), 30 mL of absolute ethanol, hydrazine hydrate (1 mL, 21 mmol), and Pd/C (87 mg, 0.42), respectively, were added to the flask. After two hours of refluxing, the mixture was cooled to room temperature. The organic phase was obtained after filtration and then concentrated with a rotary evaporator. An ethyl acetate/petroleum ether 1/1 eluent was used to purify the crude product with a silica gel column. Compound 3 was obtained as a yellow powder with an 87% yield (0.77 g). Mp $216.4\text{--}218.6\text{ }^{\circ}\text{C}$; IR (KBr) ν 3460, 3414, 3363, 3024, 2835, 1605, 1508, 1443, 1238, 1172, 1026, 833 cm^{-1} ; ^1H NMR (400 MHz, DMSO) δ 6.46 (d, $J = 8.4\text{ Hz}$, 4H), 6.63 (d, $J = 8.4\text{ Hz}$, 4H), 6.56 (d, $J = 8.0\text{ Hz}$, 4H), 6.24 (d, $J = 8.0\text{ Hz}$, 4H), 4.92 (s, 4H), 3.64 (s, 6H) ppm; ^{13}C NMR (100 MHz, DMSO) δ : 156.9, 146.7, 139.9, 137.4, 134.6, 132.0, 131.7, 131.6, 113.1, 113.0 ppm; MS m/z calcd for $\text{C}_{28}\text{H}_{26}\text{N}_2\text{O}_2$ 422.5 [M], found 423.2055 [M^+].

4. Conclusions

In conclusion, this paper presented the design and synthesis of an aggregation-induced emission fluorescent sensor for a nitrophenolic explosives in aqueous media, which was highly effective. The fluorescence quenching of the sensor was observed due to the formation of the 1: 2 complex with TNP/DNP. The binding constants of compound 3 with TNP and DNP were calculated to be 3.4×10^8 and 7.4×10^7 , respectively. This simple sensor exhibited high potential for the detection of TNP and DNP both in water and in the solid state.

Supplementary Materials: The following supporting information can be downloaded at: <https://www.mdpi.com/article/10.3390/molecules28010181/s1>, Figures S1–S4: characteristic spectra; Figure S5: UV/vis spectra; Figure S6: SEM images; Figures S7–S11: fluorescence spectra.

Author Contributions: Conceptualization, D.L. and H.-T.F.; methodology, D.L. and P.L.; validation, X.-W.H., Z.J. and M.Z.; writing—original draft preparation, D.L.; writing—review and editing, H.-T.F. All authors have read and agreed to the published version of the manuscript.

Funding: This work was supported by the National Natural Science Foundation of China (52173152, 21805002), Guangdong Basic and Applied Basic Research Foundation (2020A1515110476), the Fund of the Rising Stars of Shaanxi Province (2021KJXX-48), Scientific Research Program Funded by Shaanxi Provincial Education Department (22JK0247), Scientific and Technological Innovation Team of Shaanxi Province (2022TD-36).

Institutional Review Board Statement: Not applicable.

Informed Consent Statement: Not applicable.

Data Availability Statement: Not applicable.

Conflicts of Interest: The authors declare no conflict of interest.

Sample Availability: Samples of the compounds are not available from the authors.

References

1. Patil, G.; Dongre, S.-D.; Das, T. Sukumaran. S.-B. Dual Mode Selective Detection and Differentiation of TNT from Other Nitroaromatic Compounds. *J. Mater. Chem. A* **2020**, *8*, 10767–10771.
2. Shanmugaraju, S.; Dabadie, C.; Byrne, K.; Savyasachi, A.-J.; Umadevi, D.; Schmitt, W.; Kitchen, J.-A.; Gunnlaugsson, T. A supramolecular Tröger's base derived coordination zinc polymer for fluorescent sensing of phenolic-nitroaromatic explosives in water. *Chem. Sci.* **2017**, *8*, 1535–1546. [[CrossRef](#)] [[PubMed](#)]
3. Danquah, M.-K.; Wang, S.; Wang, Q.-Y.; Wang, B.; Wilson, L.-D. A porous β -cyclodextrin-based terpolymer fluorescence sensor for in situ trinitrophenol detection. *RSC Adv.* **2019**, *9*, 8073–8080. [[CrossRef](#)] [[PubMed](#)]
4. Forbes, T.-P.; Sisco, E. Recent advances in ambient mass spectrometry of trace explosives. *Analyst* **2018**, *143*, 1948–1969. [[CrossRef](#)]
5. Abhiram, P.; Basanta, P.-S.; Sonam, M.; Debasis, N.; Santanab, G.; Tridib, K.-S. AIE active fluorescent organic nanoaggregates for selective detection of phenolic-nitroaromatic explosives and cell imaging. *J. Photoch. Photobio. A* **2019**, *374*, 194–205.
6. Marder, D.; Tzanani, N.; Prihed, H.; Gura, S. Trace detection of explosives with a unique large volume injection gas chromatography-mass spectrometry (LVI-GC-MS) method. *Anal. Methods* **2018**, *10*, 2712–2721. [[CrossRef](#)]
7. Mu, R.; Shi, H.; Yuan, Y.; Karnjanapiboonwong, A.; Burken, J.-G.; Ma, Y. Fast separation and quantification method for nitroguanidine and 2,4-dinitroanisole by ultrafast liquid chromatography–tandem mass spectrometry. *Anal. Chem.* **2012**, *84*, 3427–3432. [[CrossRef](#)]
8. Najarro, M.; Dávila Morris, M.-E.; Staymates, M.-E.; Fletcher, R.; Gillen, G. Optimized thermal desorption for improved sensitivity in trace explosives detection by ion mobility spectrometry. *Analyst* **2012**, *137*, 2614–2622. [[CrossRef](#)] [[PubMed](#)]
9. Singh, S.; Meena, V.-K.; Mizaikoff, B.; Singh, S.-P.; Suri, C.-R. Electrochemical sensing of nitro-aromatic explosive compounds using silver nanoparticles modified electrochips. *Anal. Methods* **2016**, *8*, 7158–7169. [[CrossRef](#)]
10. Babae, S.; Beiraghi, A. Micellar extraction and high performance liquid chromatography-ultra violet determination of some explosives in water samples. *Anal. Chim. Acta* **2010**, *662*, 9–13. [[CrossRef](#)]
11. Jha, S.-K.; Ekinci, Y.; Agio, M.; Löffler, J.-F. Towards deep-UV surface-enhanced resonance Raman spectroscopy of explosives: Ultrasensitive, real-time and reproducible detection of TNT. *Analyst* **2015**, *140*, 5671–5677. [[CrossRef](#)]
12. Salinas, Y.; Martinez-Manez, R.; Marcos, M.-D.; Sancenon, F.; Costero, A.-M.; Parra, M.; Gil, S. Optical chemosensors and reagents to detect explosives. *Chem. Soc. Rev.* **2012**, *41*, 1261–1296. [[CrossRef](#)] [[PubMed](#)]
13. Shanmugaraju, S.; Mukherjee, P.-S. π -Electron rich small molecule sensors for the recognition of nitroaromatics. *Chem. Commun.* **2015**, *51*, 16014–16032. [[CrossRef](#)] [[PubMed](#)]
14. Sun, X.; Wang, Y.; Lei, Y. Fluorescence based explosive detection: From mechanisms to sensory materials. *Chem. Soc. Rev.* **2015**, *44*, 8019–8061. [[CrossRef](#)] [[PubMed](#)]
15. Wu, X.-X.; Fu, H.-R.; Han, M.-L.; Zhou, Z.; Ma, L.-F. Tetraphenylethylene immobilized metal-organic frameworks: Highly sensitive fluorescent sensor for the detection of $\text{Cr}_2\text{O}_7^{2-}$ and nitroaromatic explosives. *Cryst. Growth Des.* **2017**, *17*, 6041–6048. [[CrossRef](#)]
16. Dang, R.; Ma, X.-R.; Zhao, Y.-P.; Ren, M.; Guo, W.; Kang, Y.-H.; Gao, Y.; Bi, S.; Gao, W.; Hao, H.-R.; et al. Construction of 3D Ni^{2+} - Al^{3+} -LDH/ γ - Fe_2O_3 - Cd^{2+} - Ni^{2+} - Fe^{3+} -LDH structures and multistage recycling treatment of dye and fluoride-containing wastewater. *Chem. Eng. J.* **2023**, *451*, 138499. [[CrossRef](#)]
17. Nabeel, F.; Rasheed, T.; Mahmood, M.-F.; Khan, S.-U.-D. Hyperbranched copolymer based photoluminescent vesicular probe conjugated with tetraphenylethene: Synthesis, aggregation-induced emission and explosive detection. *J. Mol. Liq.* **2020**, *308*, 113034–113042. [[CrossRef](#)]
18. Liu, S.-G.; Luo, D.; Li, N.; Zhang, W.; Lei, J.-L.; Li, N.-B.; Luo, H.-Q. Water-Soluble Nonconjugated Polymer Nanoparticles with Strong Fluorescence Emission for Selective and Sensitive Detection of Nitro-Explosive Picric Acid in Aqueous Medium. *ACS Appl. Mater. Interfaces* **2016**, *8*, 21700–21709. [[CrossRef](#)]
19. Hu, Z.; Deibert, B.-J.; Li, J. Luminescent metal-organic frameworks for chemical sensing and explosive detection. *Chem. Soc. Rev.* **2014**, *43*, 5815–5840. [[CrossRef](#)]
20. Zhao, Y.; Ma, Y.; Li, H.; Wang, L. Composite QDS@MIP nanospheres for specific recognition and direct fluorescent quantification of pesticides in aqueous media. *Anal. Chem.* **2012**, *84*, 386–395. [[CrossRef](#)]
21. Liu, B.; Tong, C.; Feng, L.; Wang, C.; He, Y.; Lü, C. Water-soluble polymer functionalized CdTe/ZnS quantum dots: A facile ratiometric fluorescent probe for sensitive and selective detection of nitroaromatic explosives. *Chem. Eur. J.* **2014**, *20*, 2132–2137. [[CrossRef](#)] [[PubMed](#)]
22. Luo, J.; Xie, Z.; Lam, J.W.-Y.; Cheng, L.; Chen, H.; Qiu, C.; Kwok, H.-S.; Zhan, X.; Liu, Y.; Zhu, D.; et al. Aggregation-induced emission of 1-methyl-1,2,3,4,5-pentaphenylsilole. *Chem. Commun.* **2001**, *18*, 1740–1741. [[CrossRef](#)] [[PubMed](#)]
23. Zhao, E.-G.; Chen, Y.-L.; Chen, S.-J.; Deng, H.-Q.; Gui, C.; Leung, C.-W.-T.; Hong, Y.-N.; Lam, J.-W.-Y.; Tang, B.-Z. A luminogen with aggregation-induced emission characteristics for wash-free bacterial imaging, high-throughput antibiotics screening and bacterial susceptibility evaluation. *Adv. Mater.* **2015**, *27*, 4931–4937. [[CrossRef](#)] [[PubMed](#)]
24. Niu, G.-L.; Zheng, X.-L.; Zhao, Z.; Zhang, H.-K.; Wang, J.-G.; He, X.-W.; Chen, Y.-C.; Shi, X.-J.; Ma, C.; Kwok, R.-T.-K.; et al. Functionalized acrylonitriles with aggregation-induced emission: Structure tuning by simple reaction-condition variation, efficient red emission, and two-photon bioimaging. *J. Am. Chem. Soc.* **2019**, *141*, 15111–15120. [[CrossRef](#)] [[PubMed](#)]
25. Gao, M.; Tang, B.-Z. Fluorescent sensors based on aggregation-induced emission: Recent advances and perspectives. *ACS Sens.* **2017**, *2*, 1382–1399. [[CrossRef](#)]

26. Zhang, J.; Liu, Q.-M.; Wu, W.-J.; Peng, J.-H.; Zhang, H.-K.; Song, F.-Y.; He, B.-Z.; Wang, X.-Y.; Sung, H.H.-Y.; Chen, M.; et al. Real-time monitoring of hierarchical self-assembly and induction of circularly polarized luminescence from achiral luminogens. *ACS Nano* **2019**, *13*, 3618–3628. [[CrossRef](#)]
27. Kwok, R.T.K.; Leung, C.W.T.; Lam, J.W.Y.; Tang, B.Z. Biosensing by luminogens with aggregation-induced emission characteristics. *Chem. Soc. Rev.* **2015**, *44*, 4228–4238. [[CrossRef](#)]
28. Wang, J.-H.; Feng, H.-T.; Zheng, Y.-S. Synthesis of tetraphenylethylene pillar[6]arenes and the selective fast quenching of their AIE fluorescence by TNT. *Chem. Commun.* **2014**, *50*, 11407–11410. [[CrossRef](#)]
29. Che, W.; Li, G.; Liu, X.; Shao, K.; Zhu, D.; Su, Z.; Bryce, M.-R. Selective sensing of 2,4,6-trinitrophenol (TNP) in aqueous media with “aggregation-induced emission enhancement” (AIEE)-active iridium(III) complexes. *Chem. Commun.* **2018**, *54*, 1730–1733. [[CrossRef](#)]
30. Zhou, H.; Chua, M.-H.; Tang, B.-Z.; Xu, J. Aggregation-induced emission (AIE)-active polymers for explosive detection. *Polym. Chem.* **2019**, *10*, 3822–3840. [[CrossRef](#)]
31. Delente, J.M.; Umadevi, D.; Shanmugaraju, S.; Kotova, O.; Watson, G.W.; Gunnlaugsson, T. Aggregation induced emission (AIE) active 4-amino-1,8-naphthalimide-Tröger’s base for the selective sensing of chemical explosives in competitive aqueous media. *Chem. Commun.* **2020**, *56*, 2562–2565. [[CrossRef](#)] [[PubMed](#)]
32. Prusti, B.; Chakravarty, M. An electron-rich small AIEgen as a solid platform for the selective and ultrasensitive on-site visual detection of TNT in the solid, solution and vapor states. *Analyst* **2020**, *145*, 1687–1694. [[CrossRef](#)] [[PubMed](#)]
33. Yuan, W.-Z.; Zhao, H.; Shen, X.-Y.; Mahtab, F.; Lam, J.-W.-Y.; Sun, J.-Z.; Tang, B.-Z. Luminogenic Polyacetylenes and Conjugated Polyelectrolytes: Synthesis, Hybridization with Carbon Nanotubes, Aggregation-Induced Emission, Superamplification in Emission Quenching by Explosives, and Fluorescent Assay for Protein Quantitation. *Macromolecules* **2009**, *42*, 9400–9411. [[CrossRef](#)]
34. Hu, R.; Maldonado, J.-L.; Rodriguez, M.; Deng, C.; Jim, C.-K.-W.; Lam, J.-W.-Y.; Yuen, M.-M.-F.; Ramos-Ortiz, G.; Tang, B.-Z. Luminogenic materials constructed from tetraphenylethylene building blocks: Synthesis, aggregation-induced emission, two-photon absorption, light refraction, and explosive detection. *J. Mater. Chem.* **2012**, *22*, 232–240. [[CrossRef](#)]
35. Qin, A.; Lam, J.-W.-Y.; Tang, L.; Jim, C.-K.-W.; Zhao, H.; Sun, J.; Tang, B.-Z. Polytriazoles with Aggregation-Induced Emission Characteristics: Synthesis by Click Polymerization and Application as Explosive Chemosensors. *Macromolecules* **2009**, *42*, 1421–1424. [[CrossRef](#)]
36. Liu, J.; Zhong, Y.; Lam, J.-W.-Y.; Lu, P.; Hong, Y.; Yu, Y.; Yue, Y.; Faisal, M.; Sung, H.-H.-Y.; Williams, I.-D.; et al. Hyperbranched Conjugated Polysiloles: Synthesis, Structure, Aggregation-Enhanced Emission, Multicolor Fluorescent Photopatterning, and Superamplified Detection of Explosives. *Macromolecules* **2010**, *43*, 4921–4936. [[CrossRef](#)]
37. Feng, H.-T.; Zheng, Y.-S. Highly Sensitive and Selective Detection of Nitrophenolic Explosives by Using Nanospheres of a Tetraphenylethylene Macrocycle Displaying Aggregation-Induced Emission. *Chem. Eur. J.* **2014**, *20*, 195–201. [[CrossRef](#)] [[PubMed](#)]
38. Feng, H.-T.; Wang, J.-H.; Zheng, Y.-S. CH₃– π Interaction of Explosives with Cavity of a TPE Macrocycle: The Key Cause for Highly Selective Detection of TNT. *ACS Appl. Mater. Interfaces* **2014**, *6*, 20067–20074. [[CrossRef](#)]
39. Xiong, J.-B.; Wang, J.-H.; Li, B.; Zhang, C.; Tan, B.; Zheng, Y.-S. Porous Interdigitation Molecular Cage from Tetraphenylethylene Trimeric Macrocycles That Showed Highly Selective Adsorption of CO₂ and TNT Vapor in Air. *Org. Lett.* **2018**, *20*, 321–324. [[CrossRef](#)]
40. Li, D.; Zhang, T.; Ji, B. Influences of pH, urea and metal ions on the interaction of sinomenine with Lysozyme by steady state fluorescence spectroscopy. *Spectrochim. Acta Part A* **2014**, *130*, 440–446. [[CrossRef](#)]
41. Li, D.; Yang, Y.; Cao, X.; Xu, C.; Ji, B. Investigation on the pH-dependent binding of vitamin B12 and lysozyme by fluorescence and absorbance. *J. Mol. Struct.* **2012**, *1007*, 102–112. [[CrossRef](#)]

Disclaimer/Publisher’s Note: The statements, opinions and data contained in all publications are solely those of the individual author(s) and contributor(s) and not of MDPI and/or the editor(s). MDPI and/or the editor(s) disclaim responsibility for any injury to people or property resulting from any ideas, methods, instructions or products referred to in the content.